



Transient recovery of epicardial and torso ST-segment ischemic signals during cardiac stress tests: A possible physiological mechanism

Brian Zenger^{a,b,c,d,*}, Wilson W. Good^{a,b,c}, Jake A. Bergquist^{a,b,c}, Lindsay C. Rupp^{a,b,c}, Maura Perez^a, Gregory J. Stoddard^e, Vikas Sharma^d, Rob S. MacLeod^{a,b,c}

^a Scientific Computing and Imaging Institute, University of Utah, SLC, UT, USA

^b Nora Eccles Harrison Cardiovascular Research and Training Institute, University of Utah, SLC, UT, USA

^c Department of Biomedical Engineering, University of Utah, SLC, UT, USA

^d School of Medicine, University of Utah, SLC, UT, USA

^e Department of Internal Medicine, University of Utah, SLC, UT, USA

ARTICLE INFO

Article history:

Received 14 May 2021

revised 24 June 2021

accepted 6 July 2021

Keywords:

Acute myocardial ischemia

Cardiac stress test

Experimental model

ST-segment changes

ABSTRACT

Background: Acute myocardial ischemia has several characteristic ECG findings, including clinically detectable ST-segment deviations. However, the sensitivity and specificity of diagnosis based on ST-segment changes are low. Furthermore, ST-segment deviations have been shown to be transient and spontaneously recover without any indication the ischemic event has subsided.

Objective: Assess the transient recovery of ST-segment deviations on remote recording electrodes during a partial occlusion cardiac stress test and compare them to intramyocardial ST-segment deviations.

Methods: We used a previously validated porcine experimental model of acute myocardial ischemia with controllable ischemic load and simultaneous electrical measurements within the heart wall, on the epicardial surface, and on the torso surface. Simulated cardiac stress tests were induced by occluding a coronary artery while simultaneously pacing rapidly or infusing dobutamine to stimulate cardiac function. Postexperimental imaging created anatomical models for data visualization and quantification. Markers of ischemia were identified as deviations in the potentials measured at 40% of the ST-segment. Intramural cardiac conduction speed was also determined using the inverse gradient method. We assessed changes in intramyocardial ischemic volume proportion, conduction speed, clinical presence of ischemia on remote recording arrays, and regional changes to intramyocardial ischemia. We defined the peak deviation response time as the time interval after onset of ischemia at which maximum ST-segment deviation was achieved, and ST-recovery time was the interval when ST deviation returned to below threshold of ST elevation.

Results: In both epicardial and torso recordings, the peak ST-segment deviation response time was 4.9 ± 1.1 min and the ST-recovery time was approximately 7.9 ± 2.5 min, both well before the termination of the ischemic stress. At peak response time, conduction speed was reduced by 50% and returned to near baseline at ST-recovery. The overall ischemic volume proportion initially increased, on average, to 37% at peak response time; however, it recovered to only 30% at the ST-recovery time. By contrast, the subepicardial region of the myocardial wall showed 40% ischemic volume at peak response time and recovered much more strongly to 25% as epicardial ST-segment deviations returned to baseline.

Conclusion: Our data show that remote ischemic signal recovery correlates with a recovery of the subepicardial myocardium, whereas subendocardial ischemic development persists.

© 2021 Elsevier Inc. All rights reserved.

Introduction

Chest pain is the most common patient complaint when arriving at the emergency department, with acute myocardial ischemia being the most worrisome underlying cause [1,2]. During the clinical assessment,

patients receive an electrocardiogram (ECG) to measure the electrical activity of the heart and identify ECG signal deviations typical of ischemia. However, ECG signals indicating acute myocardial ischemia are transient and may not detect ischemia despite an event occurring [3,4]. Previously, the disappearance of these ischemic ECG signals was interpreted to mean the ischemic event had ended and the cardiac tissue was recovering. However, detailed studies have shown, despite the decreasing or absent ischemic ECG markers, that ischemia within the myocardium may persist

* Corresponding author at: 72 South Campus Dr., SLC, UT 84112, USA.
E-mail address: brian.zenger@hsc.utah.edu (B. Zenger).

[3,4]. Without intervention, the myocardium will continue to degrade, leading to cell death and significant long-term risks of increased morbidity and mortality [5]. Therefore, we need to understand the evolution and progression of remotely recorded ischemic signals related to underlying ischemic myocardial substrates and the possible mechanisms that lead to decreased ischemic ECG signals.

Many previous experimental and clinical studies have shown the transient disappearance of ischemic ECG signals during a controlled ischemic event [6–8]. During an ischemic episode, ST-segment deviations in the ECG signals initially increase, accompanied by a significant increase in arrhythmic events such as premature ventricular contractions or other re-entrant-type arrhythmic patterns [6,8]. Following this initial phase, which can last up to 15 min, ST-segment deviations and arrhythmic events decrease significantly, indicating apparent myocardial recovery even as the critically reduced myocardial perfusion persists [6,8]. This persistence is apparent only under closer examination of the myocardial tissue (possible only in experiments), which can show ischemia at the cellular level, with consequences that include cell-to-cell uncoupling [9]. This uncoupling reduces passive current flow between cells and eliminates the ST-segment deflections recorded on remote electrodes [9]. Furthermore, cell-to-cell uncoupling leads to significant conduction velocity slowing, which can be monitored and characterized in an experimental preparation as a temporal spreading of the QRS complex and prolongation of activation times [10].

The studies discussed above have shown this transient recovery only during ischemia induced by complete occlusion of the coronary artery. They did not report changes during a partial occlusion event or added cardiac stress, such as experienced during a cardiac stress test. Partial occlusion ischemia has markedly different effects than complete occlusion ischemia, including the nontransmural distribution of ischemic regions [11]. Partial occlusion ischemia is induced and detected using cardiac stress tests, which stimulate the heart via regulated exercise or drug infusion to expose regional perfusion deficits to cardiac tissue [12,13]. As ischemia develops, key biomarkers are monitored for responses, including changes to the ST-segment of electrocardiograms [12,13]. Previously reported studies of partial occlusion myocardial ischemia have lacked the high-resolution and multidomain recording that would enable a comprehensive analysis of the transient changes in ischemic electrical signals throughout the myocardium, on the epicardial surface, and on the torso surface. We set out to address this deficit through experiments focused on comprehensive monitoring of acute, nontransmural ischemia.

This study aimed to examine the transient recovery of ischemic signals during a simulated cardiac stress test with partial flow ischemia. We used a previously validated experimental model of partial occlusion acute myocardial ischemia, instrumented with electrode arrays within the myocardium, on the epicardial surface, and on the torso surface to examine this recovery phenomenon. We controlled ischemic stress using hydraulic occlusion with pacing or pharmacological stimulation. We then assessed several different ischemia metrics, including typical ST-segment deviations, changes in intramyocardial conduction speed, and regional recovery of ischemic electrical signals. Our results showed a significant recovery of epicardial and torso surface ischemic ST-segment potentials during each episode of simulated cardiac stress test, i.e., even while the stress level increased. Using conduction speed measurements, we found no evidence that this recovery was related to cell-to-cell uncoupling. Furthermore, we identified preferential recovery of ischemic potentials in the subepicardial myocardial tissue.

Methods

Experimental model

The experimental model used in this study has been described previously in Zenger et al. [14]. In short, midline sternotomies were performed on anesthetized 30 Kg male or female Yucatan minipigs to

expose the anterior cardiac surface. Each animal was instrumented with intramural, epicardial, and torso surface electrode arrays. Intramural arrays were custom-fabricated plunge needles with 10 individual recording electrodes spaced 1.6 mm down the needle shaft. For each experiment, 20–30 needles were placed in the approximate left anterior descending coronary artery (LAD) perfusion bed with an approximate interneedle spacing of 5–10 mm at the epicardium. A 247-electrode epicardial sock array was placed around the ventricular epicardium with approximately 6.6 mm² electrode resolution and approximately 10 mm spacing between electrodes. After instrumentation, the chest wall was closed with sutures, and residual air was evacuated. Torso electrode strips, each with 12 electrodes spaced 3 cm apart, were placed from superior to inferior across the animal torso with 8–12 strips spanning around the thorax. All signals were low-pass filtered, gain adjusted, and sampled simultaneously with a custom digital multiplexer at 1 kHz [15]. All animals were purpose-bred for use in experimental research. All studies were approved by the Institutional Animal Care and Use Committee at the University of Utah and conformed to the Guide for Care and Use of Laboratory Animals (protocol number 17-04016 approved on 05/17/2017).

Quantification of ischemia

Signals were processed and filtered using the PFEIFER open-source ECG and electrogram annotation suite [16]. Signals with low signal-to-noise values were manually identified and removed from intramural recordings or reconstructed via Laplacian interpolation from the surrounding electrodes on the epicardial and torso surfaces. ST-segment changes were used as indicators for acute myocardial ischemia. From each beat, we extracted the potential value at 40% into the ST-segment duration (from the end of the QRS to peak of the T wave) and averaged the values over a ± 5 ms time frame. Representative ST40% potentials were extracted every 15 s from continuously acquired data throughout the experiment.

Simulated cardiac stress test

Controlled cardiac stress was induced by limiting coronary perfusion and increasing cardiac activity. A calibrated hydraulic occluder was placed around the left anterior descending coronary artery (LAD) to reduce perfusion. The occluder could then be adjusted from 0 to 100% of the original cross-sectional area. Cardiac stress was induced using right atrial pacing at elevated rates or pharmacological stimulation via dobutamine infusion. Typical clinical protocols were used for target pacing and drug infusion rates [12,13]. Each episode of ischemia lasted 15 min with a fixed level of occlusion, which was determined on an experiment by experiment basis by the animal stability. Each 15-min episode was broken into five 3-min stages. After each stage, the pacing or pharmacological infusion rate was increased. A 30-min rest period followed each ischemic episode, which has been shown as adequate time for the heart to return to baseline potentials [14]. Up to four episodes were performed in each animal.

Image-based modeling pipeline

The torso geometries and electrode locations were acquired via postmortem magnetic resonance imaging (MRI) (Siemens Medical, Erlangen, Germany). We then explanted the heart and acquired submillimeter high-resolution MRI (Bruker BIOSPEC 70/30, Billerica, MA). Torso geometries, cardiac anatomy, and electrode locations were segmented using the Seg3D open-source software package (www.seg3d.org, SCI Institute, SLC, UT). The anatomical structures were meshed to create triangulated tetrahedral models using the Cleaver mesh tool (SCI Institute, SLC, UT). Geometries were registered and further refined using the GRÖMER registration pipeline [17]. Visualizations were performed using the *map3d* (www.sci.utah.edu/software/map3d) and SCIRun

(www.sci.utah.edu/software/scirun) open-source software packages and MATLAB (Mathworks, MA, USA). Measured ST40% potentials were interpolated into the intramyocardial volume using thin-plate spline radial basis functions, which assigned an ST40% potential at every node within the high-resolution mesh.

Following the anatomical model creation, each high-resolution cardiac mesh was parameterized using the Universal Ventricular Coordinate (UVC) scheme from the Cardiac Arrhythmia and Research Package (CARP) [18]. These parameterizations assigned a unique four-parameter location to each node in the mesh according to values for z , ρ , ϕ , and a parameter indicating left or right ventricle, as described previously [19]. These values could then be translated across experiments as relative positions. For this analysis, we used the ρ parameter to indicate the relative intramyocardial depth (from 0 to 1) of each node within the myocardial wall. We defined the subepicardial region and subendocardial/midmyocardial regions in terms of ρ as $\rho > 0.66$ and $\rho < 0.66$, respectively.

Three-dimensional conduction velocity measurements

Three-dimensional conduction velocity was calculated using validated techniques described previously [20]. In short, activation times were first identified from intramural plunge needle electrodes and reconstructed within the sampled region of the high-resolution cardiac mesh using thin-plate spline radial basis functions [20]. We used the inverse gradient technique to calculate conduction velocity from the interpolated activation times, which inverts the activation time gradient throughout the myocardium and takes the partial derivative on an element-wise basis. Conduction velocity was further reduced to conduction speed per element by taking the vector magnitude.

Metrics of ischemia and statistical analysis

For intramural recordings, ST40% potentials of 1 mV or larger were considered ischemic. For epicardial recordings, ST40% potentials above 2 mV or below -1 mV indicate ST-segment elevation or depression, respectively. On the torso surface, ST40% potentials above 0.05 mV or below -0.05 mV were indicative of ST-segment elevation or depression, respectively. These thresholds were used to determine the number of electrodes on the epicardial and torso surfaces considered ‘clinically detectable’ as these thresholds mimic those used in evaluating ST segments in patients.

To quantify the transient changes in ischemic ST-segment potentials, we identified the time of peak ischemic ST-segment potentials and the time of recovery of ST-segment potentials during an ischemic episode. To calculate peak and recovery ST40% response times, we identified epicardial electrodes that became positively ischemic during each episode. We then calculated the time when each such electrode was at its maximum and selected the median as the time of peak ST40% for an episode. We then determined the time when electrograms that had developed positive ischemic potentials returned to below the ischemic threshold. The median time of these recovered electrograms was chosen to represent the recovery ST40% response time per episode.

Statistical differences between metrics were compared using a random-effects multilevel regression to compensate for repeated measures within subjects. Statistical significance was defined as $p < 0.05$. The plots generated show the mean \pm the standard error unless otherwise noted. Statistical analysis was performed using STATA 16.1 stats software package (StatCorp, Texas, USA).

Results

ST-segment changes throughout a simulated cardiac stress test

Fig. 1 displays an example of a typical progression in the transient changes in epicardial electrograms and torso surface ECGs throughout

an ischemic episode. We observed an increase in ST40% potentials across a large proportion of electrodes, which peaked at approximately 6 min (peak time) and returned to near baseline levels at 12 min (recovery time) despite increasing ischemic stress (pacing rate or dobutamine level). An example of the ST40% potentials at baseline, peak, recovery, and end of the episode over each recording domain is shown in Fig. 2. The pattern of ST40% increasing to a peak and the resolving during the episode occurred consistently across all surfaces.

We observed similar trends across all six animal experiments and 15 ischemic episodes (nine dobutamine stimulation and six right atrial pacing). A summary of peak and recovery ST40% response times across all interventions is shown in Fig. 3. The average time to peak was 4.9 ± 1.1 min, and the average time to recovery was 7.9 ± 2.5 min. The separation between each time distribution was almost perfect, with the peak response times significantly lower than the recovery response times ($p < 0.05$).

The changes in clinically detectable signals on the epicardial and torso surfaces are shown in Fig. 4. At peak ST-segment response time, the numbers of leads with clinically detectable ST40% shifts were 80 of 247 epicardial and 55 of 96 on the torso surface, indicating a significant amount of clinically detectable ischemia. At the recovery ST40% response time, the number of electrodes where the clinically detectable signal could be identified returned to near baseline levels with approximately 10 epicardial electrodes and 10 torso electrodes with positive ST40% clinical signals, which indicates nearly all clinically detectable ST deviations had disappeared.

Changes in 3D conduction speed

At baseline, the average conduction speed through the sampled myocardium was approximately 1.5 ± 0.2 m/s. At peak ST-segment response time, average conduction speed dropped to approximately 0.7 ± 0.3 m/s, and at recovery ST40% response time, the conduction speed returned to approximately baseline values, 1.4 ± 0.3 m/s (Fig. 5).

Changes in ischemic zone volumes within the myocardium

At baseline, less than 5% of the sampled volume was considered ischemic. At peak ST40% response time, approximately 37% of the sampled myocardium had become ischemic, which dropped to 30% at the minimum point and stayed relatively stable through the end of the episode (Fig. 6).

We then separated the sampled myocardium into two subregions: the subepicardial and the subendocardial/midmyocardial. The ischemic volume proportion in the subendocardial/midmyocardial regions followed similar trends to those of the whole myocardial region with a 35% ischemic at peak response time and 29% at recovery response time (Fig. 7, panel (a)). The subepicardial region, however, showed a more profound recovery, peaking at approximately 40% and dropping to 25% at recovery ST40% response time, which further dropped to 23% at the end of interventions (Fig. 7, panel (b)).

Discussion

This study aimed to examine the temporal changes of ischemic ST-segment potentials during partial-flow cardiac stress tests. We identified transient recovery of ST-segment potentials on average 8 min into 15-min simulated cardiac stress tests (15 ischemic episodes across 6 animals). We examined these transient recoveries from multiple domains: intramyocardial, epicardial, and torso surface. We also measured changes in intramyocardial conduction speed and volume of tissue showing ischemic potentials. We found the complete recovery of cardiac conduction speed (a surrogate for cell-to-cell coupling) correlated with recovery of ischemic ST-segment potentials. We also found the recovery of remote (epicardial and torso surface) ischemic ST-segment potentials was associated with a regional recovery in the subepicardial

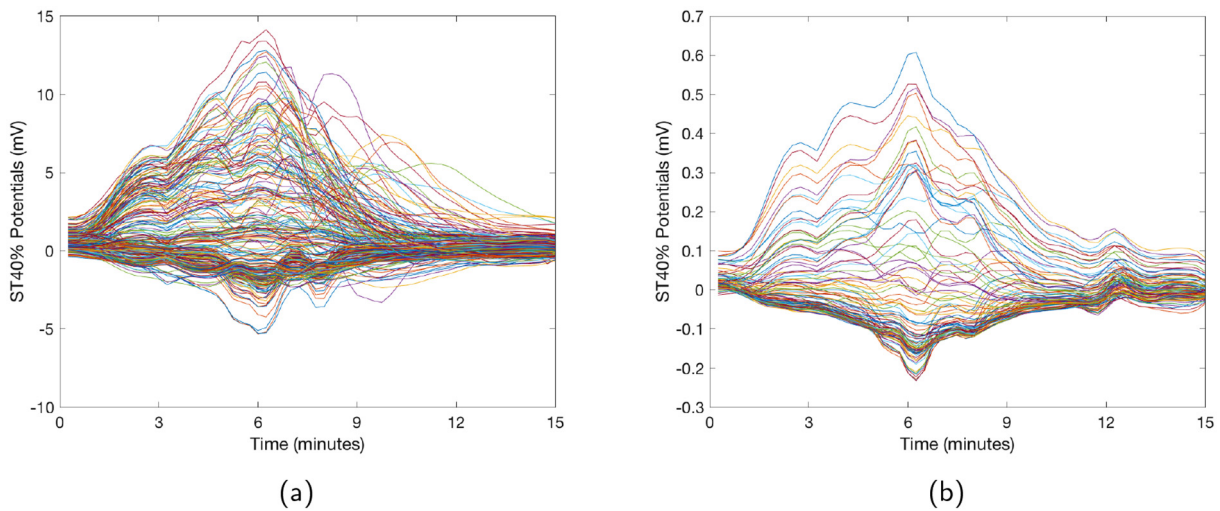


Fig. 1. Example metric plot of ST40% potential changes throughout an ischemic episode (15 min). Panel (a) shows epicardial sock ST40% potentials across all 247 electrodes. Panel (b) shows torso surface ST40% potentials across all 96 torso electrodes. Each line represents a sequence of the ST40% potential values from one electrode throughout the same ischemic episode.

myocardial tissue, whereas significant ischemia persisted within the midmyocardial and subendocardial regions.

Transient recovery of intramyocardial conduction speed during ischemic interventions

To pinpoint a possible mechanism for the transient recovery of ischemic potentials, we examined the conduction speed throughout the myocardium during ischemic stress. We found a similar recovery trend in conduction speed as in ischemic potentials on the epicardial and torso surfaces. Specifically, we observed a 50% conduction speed

decrease at the peak response time of epicardial ST40% potentials and a near-complete return to baseline conduction speeds at the recovery response time. The initial decrease in conduction speed from ischemia is well documented [10,21]. A novel finding of this study was the subsequent recovery of conduction speed, suggesting that the electrical function of the cardiomyocyte remained intact, despite persistent, hyperacute (< 15 min) ischemic stress.

The conduction speed recovery is a crucial finding to determine a possible recovery mechanism of transient ischemic potentials. Previous research in complete occlusion experimental models has shown a significant decrease in cell-to-cell coupling as the biophysical basis for

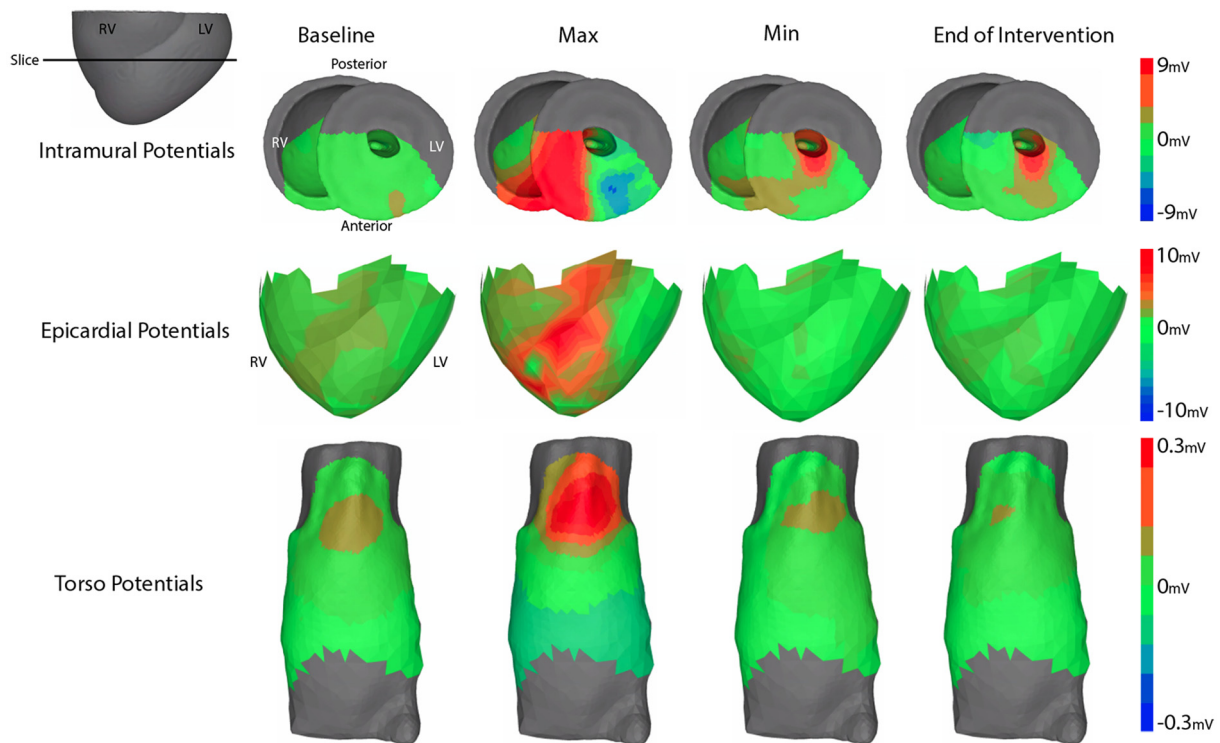


Fig. 2. Example ST40% potential values measured across all recording domains at baseline, peak ST40% response time, recovery ST40% response time, and the end of the episode, which was the time of maximal cardiac stress.

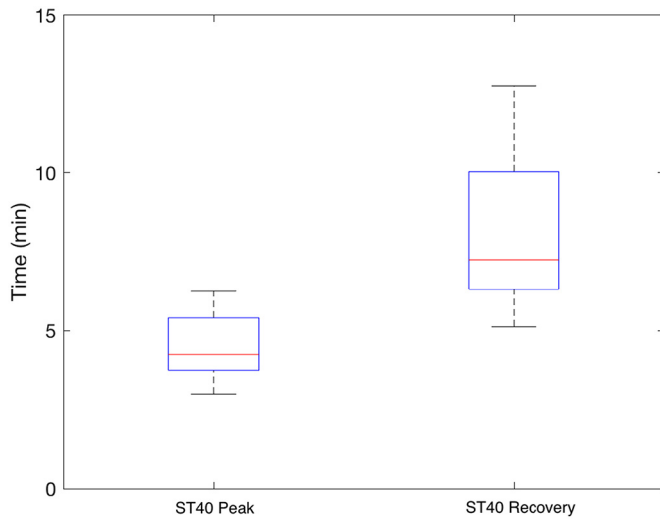


Fig. 3. Average time to peak and recovery ST40% values as measured on the epicardial sock electrodes.

the decrease in ST40% deviations [6,8,9]. Initial deviations of ST40% potentials are created by passive injury currents that flow intercellularly from healthy to ischemic tissue through gap junctions [22]. Intercellular conductance decreases significantly at some time following complete coronary occlusion, which correlates with a decrease in the ST-segment ischemic potentials. This decreased intercellular conductance decreases injury currents and results in decreased extracellular ST-segment potentials [22]. In our experimental model, which involved only reduction of coronary blood flow in the face of elevated cardiac stress, conduction speed can serve as a metric of cell-to-cell coupling because the rapid propagation of current throughout myocardial tissue is dependent on cellular coupling via gap junctions. Without cell-to-cell coupling, conduction speed has been shown to drop to near zero [6]. Our results, by contrast, show a significant recovery in conduction speed, corresponding to the recovery in ischemic potentials, which suggests cell-to-cell uncoupling is not the primary mechanism for transient recovery of ischemic signals during our simulated cardiac stress tests.

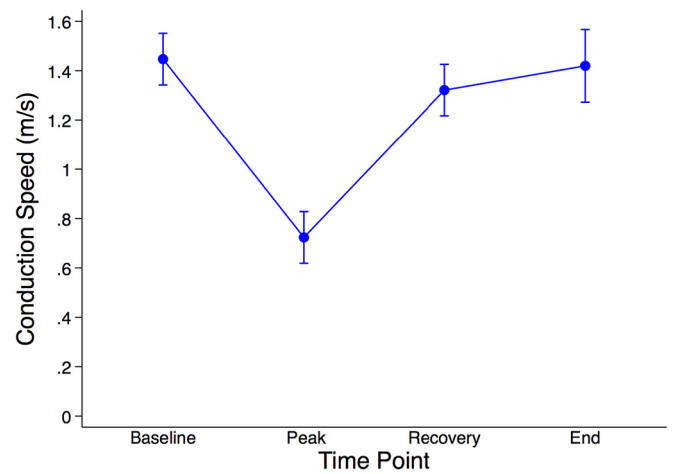


Fig. 5. Average median cardiac conduction speed measured in the myocardium at four time points, baseline, peak epicardial ST40% time, recovered epicardial ST40%, and the end of the ischemic intervention.

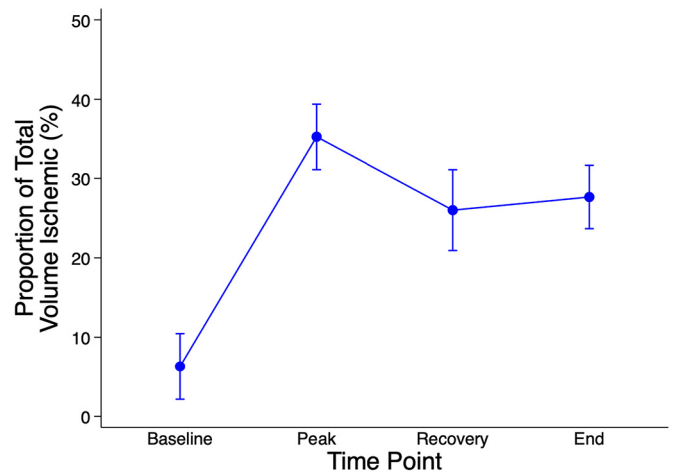
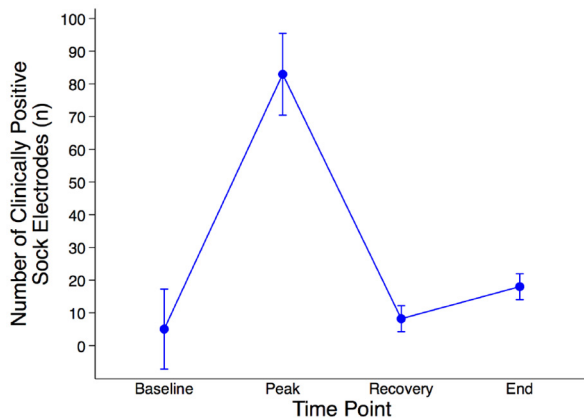
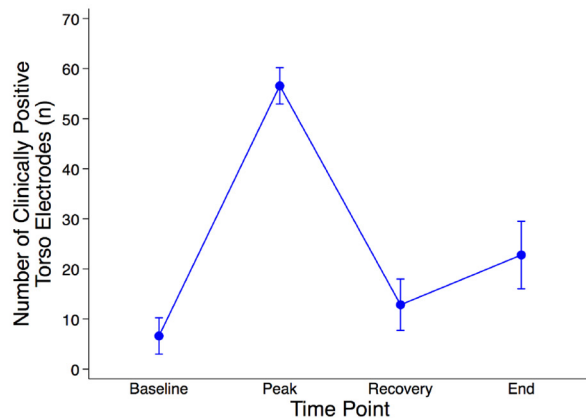


Fig. 6. Total volume proportion within the sampled myocardium that was ischemic at four time points, baseline, peak epicardial ST40% time, recovered epicardial ST40%, and the end of the ischemic intervention.



(a)



(b)

Fig. 4. Changes in measured clinically detectable signal (as either depressions or elevations) as measured on the (a) epicardial and (b) torso surfaces at four time points, baseline, peak epicardial ST40% time, recovered epicardial ST40%, and the end of the ischemic intervention at max cardiac stress.

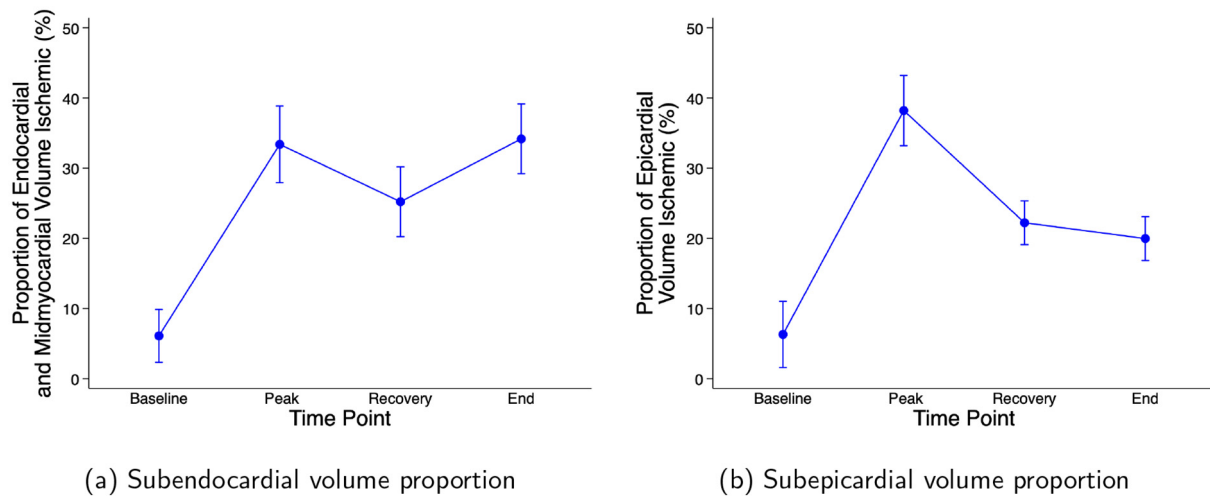


Fig. 7. Subendocardial/midmyocardial and subepicardial ischemic volume proportions at four time points, baseline, peak epicardial ST40% time, recovered epicardial ST40%, and the end of the ischemic intervention.

Differences in recovery of ischemic signals across transmural depth

We examined the changes in ischemic potentials throughout a contiguous region of the myocardial volume, which also allowed us to compare responses across the ventricular wall. We found a near-complete recovery of ST-segment potentials in the subepicardial regions but persistent ischemic zones within the midmyocardial and subendocardial regions. On the epicardium, electrodes recorded almost full recovery, suggesting that they sensed relatively healthy underlying tissue. A consequence of this epicardial recovery is that the healthy subepicardial region masks the underlying subendocardial ischemic tissue, creating a false negative marker on the epicardial surface for the presence of ischemia within the myocardium.

This subepicardial recovery impacts all remote potentials recorded from the epicardial and torso surface and provokes exploration of why this region recovers so selectively. A promising mechanism was described by Penny [23] in studies in which guinea pig hearts were Langendorff perfused, and perfusate flow was modulated between no flow and partial flow (10%). Penny observed a peak followed by a significant reduction in ischemic epicardial and action potential changes only during partial flow ischemic episodes. Penny further investigated this phenomenon and isolated catecholamine release as a possible driver for the transient restoration of normal action potentials and electrograms. Specifically, Penny noted a significant reduction in extracellular potassium concentration during the recovery phase of an acute ischemic episode, which was present only during partial-flow ischemic events. Penny also showed, during an ischemic episode, catecholamine release was associated with a simultaneous reduced extracellular potassium concentration. He hypothesized this response was from catecholamines stimulating the sodium-potassium pump, whose activity is diminished during ischemia [23]. In his experiments, removing and blocking catecholamine release suppressed the restoration of normal electrical activity that his studies (and ours) documented, which supports a hypothesis that catecholamine release is a necessary component of the transient ischemic response we observed. The time course of the observations by Penny was similar to our own, in which action potential morphology recovered at approximately 10 min into a partial flow ischemic event. These observations support the presence of a mechanism by which subepicardial recovery is driven by catecholamine release that restores the electrical state of cardiomyocytes.

Development of clinical subendocardial ischemia

Current clinical dogma of nontransmural ischemia prescribes the existence of ischemic zones that are anchored to the subendocardium,

driven strictly by differentially reduced perfusion to the subendocardial region [11,24]. This notion is substantiated by previous measurements of decreased blood flow to the subendocardial compared to the subepicardial regions. However, our studies over the past 6 years refute this notion. We have shown repeatedly that ischemia can initially develop in localized regions distributed throughout the myocardial wall, i.e., in the subepicardial, midmyocardial, or subendocardial regions [11]. This finding contradicts the clinical dogma and further blurs the notion that the electrical response to ischemia depends exclusively on levels of perfusion.

In this study, we further examined the time course of ischemia development during events that replicate a clinical cardiac stress test in a large-animal model. We showed a preferential recovery of electrical activity in the subepicardial region compared to the subendocardium and midmyocardium. This finding suggests subendocardial ischemic development is not driven solely by regional differences in blood flow but requires another critical element. The combination of our results and previous studies highlights catecholamine release as a possible additional and essential element to explain subendocardial ischemia development. Subepicardial regions likely deplete the catecholamines quickly, which prevents their protective effect from reaching the subendocardial layers. Therefore, a lack of not only nutrients but also catecholamines reaching the subendocardial regions creates a differential early recovery that appears as residual subendocardial ischemia.

A critical consequence of our findings and this proposed explanation is that recovery of electrical activity in the subepicardial region does not mean the ischemic stress has ended or that the tissue is no longer ischemic. Catecholamines in the subepicardial region have been shown to change cardiomyocyte electrical function, not rescue them from ischemic stress [23]. Previous studies have shown that significant damage still occurs within the apparently recovered ischemic tissue despite an absence of electrical indication of persistent ischemia [23]. This false recovery of ischemic potentials is another possible mechanism for the appearance of silent myocardial ischemia, which is not detected by the epicardial or other remote electrodes, i.e., body-surface ECGs.

Limitations

This study has some limitations. We do not have direct intercellular conductance measurements for cell-to-cell connectivity; however, the plethora of previous literature has documented a clear correlation between significant conduction delays and cell-to-cell uncoupling [10]. We also were unable to measure catecholamine release directly within the experimental preparation. Furthermore, the natural sympathetic and parasympathetic responses that lead to catecholamine

enhancement could have been altered by the deep anesthesia during the experiments.

Industry relationships

Dr. Wilson W. Good has recently joined the Acutus Medical Group. None of the work written or performed for this study was affected by this relationship and there is no potential conflict.

Financial support

Support for this research came from the NIH NHLBI grant no. 1F30HL149327 (Zenger); NIH NIGMS Center for Integrative Biomedical Computing (www.sci.utah.edu/cibc), NIH NIGMS grants P41GM103545 and R24GM136986 (MacLeod); the Nora Eccles Treadwell Foundation for Cardiovascular Research (MacLeod); University of Utah Population Health Research (PHR) Foundation (Stoddard); NIH NCRR and NCATS Grant no. UL1TR002538 (formerly 5UL1TR001067-05, 8UL1TR000105 and UL1RR025764) (Stoddard) No other authors have anything to disclose.

Acknowledgments

We gratefully acknowledge the support of the Nora Eccles Treadwell Cardiovascular Research and Training Institute staff, including Jayne Davis, Ala Booth, Wilson Lobaina, and Bruce Steadman, for preparing and maintaining equipment and coordinating experiment logistics.

References

- [1] Safdar B, Ong P, Camici PG. Identifying myocardial ischemia due to coronary microvascular dysfunction in the emergency department: introducing a new paradigm in acute chest pain evaluation. *Clin Ther*. 2018;1–11.
- [2] Bhuiya FA, Pitts SR, McCaig LF. Emergency department visits for chest pain and abdominal pain: United States, 1999–2008. *NCHS Data Brief*. Sept. 2010;1–8.
- [3] Cinca J, Janse MJ, Morena H, Candell J, Valle V, Durrer D. Mechanism and time course of the early electrical changes during acute coronary artery occlusion. *Chest*. 1980; 77(4):499–505.
- [4] Yan G-X, Joshi A, Guo D, Hlaing T, Martin J, Xu X, et al. Phase 2 reentry as a trigger to initiate ventricular fibrillation during early acute myocardial ischemia. *Circulation*. Aug 2004;110:1036–41.
- [5] Bairey Merz CNoel, Pepine Carl J, Walsh Mary Norine, Fleg Jerome L, Camici Paolo G, Chilian William M, Clayton Janine Austin, Cooper Lawton S, Crea Filippo, Carli Marcelo Di, Douglas Pamela S, Galis Zorina S, Gurbel Paul, Handberg Eileen M, Hasan Ahmed, Hill Joseph A, Hochman Judith S, Iturriaga Erin, Kirby Ruth, Levine Glenn N, Libby Peter, Lima Joao, Mehta Puja, Desvigne-Nickens Patrice, Olive Michelle, Pearson Gail D, Quyyumi Arshed A, Reynolds Harmony, Robinson British, Sopko George, Taqueti Viviany, Wei Janet, Wenger Nanette. Ischemia and no obstructive coronary artery disease (INOCA). *Circulation*. Mar. 2017;135:1075–92.
- [6] Degroot J, Coronel R. Acute ischemia-induced gap junctional uncoupling and arrhythmogenesis. *Cardiovasc Res*. May 2004;62:323–34.
- [7] Cinca J, Warren M, Tresanchez M, Armadans L, Gomez P, Soler-Soler J. Changes in myocardial electrical impedance induced by coronary artery occlusion in pigs with and without preconditioning: correlation with local ST-segment potential and ventricular arrhythmias. *Circ*. 1997;96:3079–86.
- [8] Kléber A, Janse M, van Capelle F, Durrer D. Mechanism and time course of ST- and TQ-segment changes during acute regional myocardial ischemia in the pig heart determined by extracellular and intracellular recordings. *Circ Res*. 1978;42:603–13.
- [9] Kléber A, Riegger C, Janse M. Electrical uncoupling and increase of extracellular resistance after induction of ischemia in isolated, arterially perfused rabbit papillary muscle. *Circ Res*. 1987;61:271–9.
- [10] Kléber A, Janse M, Wilms-Schopmann F, Wilde A, Coronel R. Changes in conduction velocity during acute ischemia in ventricular myocardium of the isolated porcine heart. *Circ*. 1986;73:189–98.
- [11] Aras K, Burton B, Swenson D, MacLeod R. Spatial organization of acute myocardial ischemia. *J Electrocardiol*. 2016;49(3):689–92.
- [12] Okin PM, Ameisen O, Kligfield P. A modified treadmill exercise protocol for computer-assisted analysis of the ST segment/heart rate slope: methods and reproducibility. *J Electrocardiol*. Oct. 1986;19:311–8.
- [13] Bartunek J, Wijns W, Heyndrickx GR, de Bruyne B. Effects of dobutamine on coronary stenosis physiology and morphology. *Circulation*. Jul 1999;100:243–9.
- [14] Zenger B, Good W, Bergquist J, Burton B, Tate J, Berkenbile L, et al. Novel experimental model for studying the spatiotemporal electrical signature of acute myocardial ischemia: a translational platform. *J Physiol Meas*. Feb 2020;41:015002.
- [15] Zenger B, Bergquist JA, Good WW, Rupp LC, MacLeod RS. High-capacity cardiac signal acquisition system for flexible, simultaneous, multidomain acquisition. *2020 Computing in cardiology*; 2020. p. 1–4.
- [16] Rodenhauer A, Good W, Zenger B, Tate J, Aras K, Burton B, et al. PFEIFER: preprocessing framework for electrograms intermittently fiducialized from experimental recordings. *J Open Source Softw*. 2018;3(21):472.
- [17] Bergquist JA, Good WW, Zenger B, Tate JD, MacLeod RS. GRÖMeR: a pipeline for geodesic refinement of mesh registration. *Lecture Notes in Computer Science. Functional Imaging and Model of the Heart (FIMH)*, Springer Verlag; 2019. p. 37–45.
- [18] Neic A, Campos FO, Prassl AJ, Niederer SA, Bishop MJ, Vigmond EJ, et al. Efficient computation of electrograms and ECGs in human whole heart simulations using a reaction-eikonal model. *J Comput Phys*. 2017;346:191–211.
- [19] Bayer J, Prassl AJ, Pashaei A, Gomez JF, Frontera A, Neic A, et al. Universal ventricular coordinates: a generic framework for describing position within the heart and transferring data. *J Med Img Anal*. 2018;45:83–93.
- [20] Good WW, Gillette K, Bergquist JA, Zenger B, Rupp LC, Tate J, et al. Estimation and validation of cardiac conduction velocity and wavefront reconstruction using epicardial and volumetric data. *IEEE transactions in biomedical engineering*; 2020 In Preparation.
- [21] Good WW, Erem B, Coll-Font J, Zenger B, Bergquist JA, Brooks D, et al. Characterizing the transient electrocardiographic signature of ischemic stress using laplacian eigenmaps for dimensionality reduction. *IEEE transactions in biomedical engineering*; 2020 In Preparation.
- [22] Russell DC, Lawrie JS, Riemersma RA, Oliver MF. Mechanisms of phase 1a and 1b early ventricular arrhythmias during acute myocardial ischemia in the dog. *Am J Cardiol*. Jan 1984;53:307–12.
- [23] Penny WJ. The deleterious effects of myocardial catecholamines on cellular electrophysiology and arrhythmias during ischaemia and reperfusion. *Eur Heart J*. Dec 1984;5:960–73.
- [24] Holland R, Brooks H. TQ-ST segment mapping: critical review and analysis of current concepts. *Am J Cardiol*. 1977;40(1):110–29.